ChemComm

Orthogonal reactivity and interface-driven selectivity during cation exchange of heterostructured metal sulfide nanorods

Journal:	*ChemComm*
Manuscript ID	CC-COM-12-2021-007190.R1
Article Type:	Communication

COMMUNICATION

Orthogonal reactivity and interface-driven selectivity during cation exchange of heterostructured metal sulfide nanorods

Received 00th January 20xx,
Accepted 00th January 20xx

DOI: 10.1039/x0xx00000x

Abigail M. Fagan,[a,†] Benjamin C. Steimle [a,†] and Raymond E. Schaak *[a,b,c]

We report predictive guidelines for the substoichiometric cation exchange of model two-component metal sulfide nanorods containing divalent cations of similar hardness. Unit cell volume changes, cation radii, solubility constants, and solid state interfaces influence selectivity during substoichiometric exchange of Cu^+ when multiple products are possible.

Cation exchange has emerged as a valuable post-synthetic modification strategy for transforming nanoparticles, including metal sulfides, into derivative materials while retaining features such as particle morphology, size, and crystal structure.[1-3] Partial cation exchange reactions, where the process is arrested before complete transformation, have become particularly powerful for designing and synthesizing highly complex heterostructured nanoparticles.[1,4-8] It is now possible to design thousands of heterostructured metal sulfide nanorods, each containing up to six distinct materials and up to 11 internal interfaces, using multiple sequential partial cation exchange reactions.[9] As an example, the Cu^+ cations of roxbyite $Cu_{1.8}S$ nanorods can be sequentially exchanged with substoichiometric amounts of Zn^{2+}, In^{3+}, Ga^{3+}, Co^{2+}, and Cd^{2+} to produce ZnS–$CuInS_2$–$CuGaS_2$–CoS–(CdS–$Cu_{1.8}S$) heterostructured nanorods.[9] At each exchange step, it is always the residual Cu^+ that exchanges for the other divalent or trivalent cations. This cation selectivitiy is the basis for the vast design space demonstrated in sequential cation exchange reactions.

Hard-soft acid-base (HSAB) interactions[10-12] are a key driving force for cation exchange. Softer cations, such as Cu^+ that has a Pearson's hardness value of 6.28,[11] bind more strongly to soft bases in solution, such as trioctylphosphine (TOP), than do harder cations such as Zn^{2+} or Cd^{2+}, which have Pearson's hardness values of 10.88 and 10.29, respectively.[11] Accordingly, Cu^+ cations can be driven out of $Cu_{1.8}S$ and into solution through favorable solvation by TOP. Concomitantly, Zn^{2+} or Cd^{2+} move from solution into the nanoparticle to replace the Cu^+.[5,8,9] The softer Cu^+ cations in $Cu_{1.8}S$ therefore exchange, exclusively and selectively, with the other harder cations due to large differences in hardness between the outgoing and incoming cations; harder cations typically do not replace similarly hard cations under the mild conditions common for cation exchange reactions. This selectivity of Cu^+ cations exchanging with harder cations such as Zn^{2+}, Cd^{2+}, Mn^{2+}, Co^{2+}, Ni^{2+}, In^{3+}, and Ga^{3+} is well known.[1-9,13-18] Reverse exchanges have also been reported: Cu^+ cations have been used to replace Mn^{2+} from MnS,[14] as well as Zn^{2+} and Cd^{2+} from ZnS and CdS, respectively.[13,19,20]

However, selective exchange among cations having *similar* hardness values, when they are present at the same time, remains largely unexplored, despite the potential for such reactivity to significantly expand the scope of accessible heterostructured nanoparticles. For example, partial Ag^+ exchange of ZnS–CdS nanorods was observed to selectively target the CdS segments to form ZnS–Ag_2S.[5] Based on hardness values alone, one would expect either Ag_2S–CdS to form or for there to be no selectivity. It is therefore evident that factors other than hardness enable selective cation exchange in heterostructured metal sulfide nanoparticles.

Here, we used selected model systems composed of two-component heterostructured metal sulfide nanorods to probe selectivity during exchange of cations having similar hardness values, as well as the influence of interfaces on cation exchange behavior. We first synthesized Janus nanorods having different combinations of ZnS, CdS, MnS, and CoS; the cations in these metal sulfides have similar Pearson's hardness values (Table 1) that are all significantly larger than that of Cu^+.[11] We then exposed these Janus nanorods to a substoichiometric Cu^+ exchange solution, using methanol as a hard Lewis base to preferentially coordinate the harder outgoing M^{2+} cations so that the Cu^+ cations can replace them in the nanorods. Having

[a] *Department of Chemistry, The Pennsylvania State University, University Park, PA, 16802, USA.*
[b] *Department of Chemical Engineering, The Pennsylvania State University, University Park, PA, 16802, USA.*
[c] *Materials Research Institute, The Pennsylvania State University, University Park, PA, 16802, USA.*
† These authors contributed equally.
Electronic Supplementary Information (ESI) available: Experimental details and additional TEM and EDS data. See DOI: 10.1039/x0xx00000x

the different metal sulfides incorporated into the same nanorods allowed us to minimize the impact of variables such as concentration and temperature gradients, kinetic effects for different metal sulfides, and differences in ligand coverage and colloidal stability.

We began by synthesizing nanorods of roxbyite $Cu_{1.8}S$,[9] which are shown in Figure S1 of the Supporting Information, and then exchanging them fully with Zn^{2+}, Cd^{2+}, Mn^{2+}, and Co^{2+} to form nanorods of wurtzite ZnS, CdS, MnS, and CoS, respectively; STEM-EDS element maps are shown in Figure 1a-d. (In the ZnS nanorod in Figure 1a, a thin band of $Cu_{1.8}S$ remains after the initial exchange with Zn^{2+}. Similar behavior has been observed before during Zn^{2+} exchange of $Cu_{1.8}S$ due to minimization of interfacial strain.[16]) We then back-exchanged with Cu^+, *i.e.* each sample of nanorods in Figure 1a-d was reacted with an excess amount of Cu^+, along with methanol, in an attempt to fully exchange back to $Cu_{1.8}S$. STEM-EDS element maps for the back-exchanged nanorods are shown in Figure 1e-h; Figure S2 shows the corresponding EDS spectra. The data in Figure 1 reveal that both CdS and MnS completely exchange back to $Cu_{1.8}S$, while ZnS and CoS only partially exchange under identical conditions. Given the identical conditions and crystal structures associated with all exchanges in Figure 1, we attribute differences in the extent and location of exchange to kinetic effects relating to slower diffusion rates in ZnS and CoS, as these two compounds have significantly smaller lattice parameters than CdS and MnS.

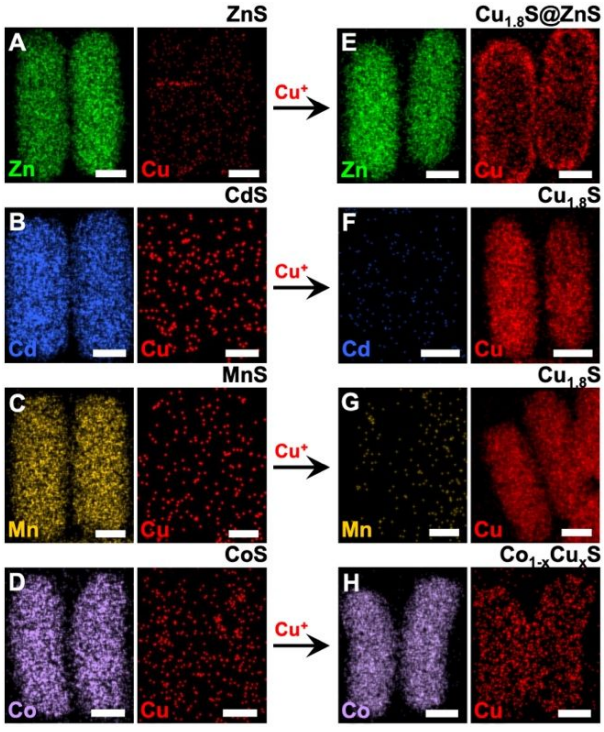

Figure 1. STEM-EDS maps for (A) ZnS, (B) CdS, (C) MnS, and (D) CoS nanorods synthesized by complete cation exchange of $Cu_{1.8}S$. (E-H) Corresponding products of attempted complete Cu^+ exchange. All scale bars are 10 nm.

We also investigated Cu^+ exchanges on a physical mixture containing equal quantities of each of the ZnS, CdS, MnS, and CoS nanorods. Here, we used enough Cu^+ to exchange approximately half of each metal cation present in the mixture. The results of this study are shown in Figure 2 (STEM-EDS maps) and Figure S3 (EDS spectra). The STEM-EDS maps reveal exchange behavior for each metal sulfide nanorod that is identical to what is shown in Figure 1. The CdS and MnS nanorods completely exchanged to $Cu_{1.8}S$, the ZnS nanorods feature a shell of $Cu_{1.8}S$, and CoS incorporates small quantities of Cu throughout the nanorod but does not exchange significantly. This competition experiment, purposely designed to have only about half of the Cu^+ cations needed to exchange all Zn^{2+}, Cd^{2+}, Mn^{2+}, and Co^{2+} cations in the physical mixture of nanorods, could have resulted in several outcomes, including half exchange of all of the nanorods or full exchange of half of the nanorods. The latter was observed, consistent with the behavior of the individual particles.

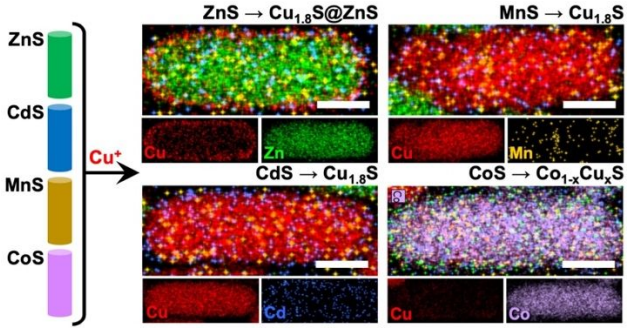

Figure 2. STEM-EDS maps from a partial Cu^+ exchange on a physical mixture of the ZnS, CdS, MnS, and CoS nanorods from Figure 1. Each type of metal sulfide nanorod appears to behave similarly to the individual exchanges in Figure 1. All scale bars 20 nm.

We then moved to Janus nanorods that contained two distinct metal sulfides in separate regions, but interfaced together. ZnS–MnS nanorods were synthesized by first performing a substoichiometric (~50%) Zn^{2+} exchange of $Cu_{1.8}S$ nanorods to produce ZnS–$Cu_{1.8}S$, followed by an exchange with Mn^{2+} in excess to ensure complete exchange of the remaining Cu^+ cations.[6,9] CdS–MnS nanorods were made similarly, using enough Cd^{2+} for a ~50% exchange to generate CdS–$Cu_{1.8}S$, followed by exchange of the remaining Cu^+ cations using excess Mn^{2+}. ZnS–CdS nanorods were synthesized using a ~50% Zn^{2+} exchange followed by a Cd^{2+} exchange in excess, and ZnS–CoS nanorods were synthesized using a ~50% Zn^{2+} exchange followed by a Co^{2+} exchange in excess. STEM-EDS element maps for each of these Janus nanorods, which represent all pairwise combinations of the four metal sulfides, are shown in Figure 3a-d; corresponding EDS spectra and wide field STEM-EDS elemental maps are shown in Figures S4 and S5, respectively. The reactions are reproducible and Figure S5 confirms that the nanorods shown in Figure 3 are representative of the sample.

Each of the nanorods in Figure 3a-d were allowed to react with a substoichiometric (~50%) amount of Cu^+. The STEM-EDS element map in Figure 3e shows that the Cu^+ exchange is selective for the CdS region of the ZnS–CdS Janus nanorods. Also, and in contrast to the data in Figures 1 and 2 for ZnS nanorods exchanging with Cu^+, there is no copper-containing shell around the ZnS, indicating that the Cu^+ cations truly are selective for the CdS region when both CdS and ZnS are present

and interfaced together in the same nanorod. ZnS–MnS and CdS–MnS Janus nanorods were exposed to a Cu^+ exchange under identical conditions. STEM-EDS maps for the products of these reactions are shown in Figure 3f and 3g; corresponding EDS data are shown in Figure S6. The Cu^+ cations appear to be selective for the MnS domain in ZnS–MnS, leaving the ZnS domain untouched. This contrasts with the behavior of ZnS by itself, where some Cu^+ exchanged with Zn^{2+}. A small amount of MnS between the ZnS and $Cu_{1.8}S$ regions is likely due to a slight deficiency of Cu^+ exchange solution available during the reaction, since the volumes are estimated based on average molecular weights,[6] or to stabilize the interface due to the large differences in unit cell volume between ZnS and $Cu_{1.8}S$ (discussed in more detail below). For the CdS–MnS nanorods, Cu^+ exchange appears to be selective for the MnS region, as a small amount of CdS remains intact (Figure 3g). While the Cu^+ over-exchanged in this case, the result hints at a progression whereby the cation for which exchange is selective reacts first, and then the other can react second if enough of the exchanging cation remains available. The $Cu_{1.8}S$–CdS nanorod in Figure 3g is particularly notable, as the residual CdS appears pinned at the original interface in the center of the Janus nanorod, such that exchange occurred around it. The morphology is unique, with a notch of CdS off-center in an otherwise $Cu_{1.8}S$ nanorod. This result highlights how selective cation exchange reactions on heterostructured precursors can be used to target unique nanostructures that would be difficult or impossible to synthesize using other methods.

Figure 3h shows a STEM-EDS map for the product of partial Cu^+ exchange of ZnS–CoS. Here, the Cu signal is localized both at the interface between the ZnS and CoS domains, as well as in a shell that surrounds that ZnS region, to form a ($Cu_{1.8}S$@ZnS)–CoS nanorod. The copper-containing shell around ZnS matches the behavior observed for Cu^+ exchange of ZnS by itself, and the copper sulfide band at the interface between ZnS and CoS nanorods made through cation exchange has been observed previously.[17] The CoS region appears to be largely untouched, and does not contain the small amount of Cu that was observed for Cu^+ exchange of CoS nanorods by themselves.

Based on the experiments and observations described above, we can now begin to rationalize the selective Cu^+ exchange behavior in the presence of similarly hard cations. Cu^+ exchange reactions on the Janus nanorods produced ZnS–$Cu_{1.8}S$ (from ZnS–MnS and ZnS–CdS), $Cu_{1.8}S$–CdS (from MnS–CdS), and ($Cu_{1.8}S$@ZnS)–CoS (from ZnS–CoS). For partial cation exchange reactions of $Cu_{1.8}S$ nanorods, it is known that the preferred interfaces are those that have the most closely matched lattice spacings.[5,9] For ZnS and $Cu_{1.8}S$, the interface perpendicular to the length of the nanorod aligns the *a*-*b* plane (in the x-y direction, with *a* and *b* being equivalent in a hexagonal cell) of both ZnS (a = 3.81 Å) and the pseudohexagonal subcell of $Cu_{1.8}S$ (a = 3.87 Å). For CdS and $Cu_{1.8}S$, the interface parallel to the length of the nanorod is preferred, as it results in optimal lattice matching in the *c*-axis direction (CdS, c = 6.72 Å, and pseudohexagonal $Cu_{1.8}S$, c = 6.71 Å). Coming back to the Cu^+ exchange reactions on the Janus nanorods, all products result in the formation of these optimal interfaces. Those that form ZnS–$Cu_{1.8}S$ align the preferred *a*-axis directions, the one that forms $Cu_{1.8}S$–CdS retains the preferred *c*-axis interface, and the one that forms ($Cu_{1.8}S$@ZnS)–CoS interfaces $Cu_{1.8}S$ and ZnS primarily along the *a*-axis direction. This analysis suggests that selectivity is driven, at least in part, by formation of optimal interfaces in the product to minimize strain by achieving the best lattice matching. The idea that interfaces play a role in selectivity during cation exchange is unexpected and differentiates the cation exchange behavior of heterostructured nanorods from those of their non-heterostructured counterparts.

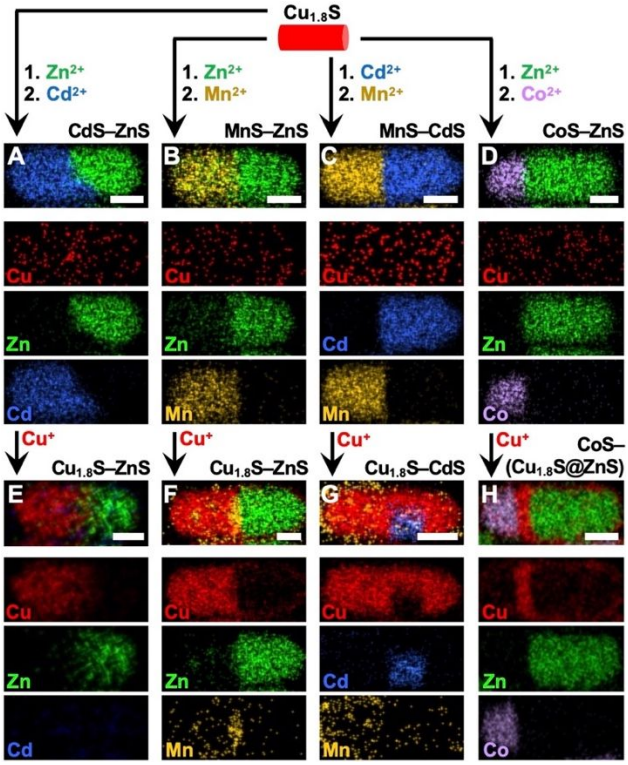

Figure 3. Combined and individual STEM-EDS maps for (A) CdS–ZnS, (B) MnS–ZnS, (C) MnS–CdS, and (D) CoS–ZnS Janus nanorods synthesized through sequential partial cation exchange reactions of $Cu_{1.8}S$ and (E-H) the corresponding products of partial cation exchange. The cation exchange behavior for these interfaced metal sulfides differs from that of the individual nanorods and their physical mixture in Figures 1 and 2. All scale bars are 10 nm.

Other considerations may also be helpful in rationalizing the observed selectivity during Cu^+ exchange of similarly hard cations. For example, based on our observations, unit cell compression is generally more favorable than unit cell expansion, perhaps due to diffusion considerations, as diffusion of larger cations (to facilitate expansion) into a smaller and more compressed unit cell would be more difficult than diffusing smaller cations into a larger and more expanded unit cell. This would, necessarily, favor unit cell compression as an outcome of a cation exchange process. This rationale is consistent with the observed behavior for three of the Janus nanorods. The unit cell volumes for CoS, ZnS, MnS, and CdS, which are based on published lattice parameters,[5,8,18] as well as the pseudohexagonal subcell of $Cu_{1.8}S$,[5] are listed in Table 1. The differences in unit cell volumes are consistent with the hypothesis that an overall unit cell compression is favorable

over a unit cell expansion during the exchange process, and that minimal unit cell compression, rather than a large overall compression, is even more favored. The order in which the metal sulfides are listed in Table 1 represents a progression from unit cell volume compression to expansion; the most favorable of those are in the middle, as they have minimal differences relative to $Cu_{1.8}S$. For ZnS–MnS and ZnS–CdS, ZnS has the smaller unit cell volume, and the component with the larger unit cell volume is the one that selectively exchanges with Cu^+. For ZnS–CoS, both have similar unit cell volumes and require large unit cell expansions, and neither exchanges significantly. For MnS–CdS, the MnS domain (the smaller unit cell) exchanges first, consistent with minimal volume compression being more favorable.

Trends in ionic radii for each cation (Table 1) are also consistent with those of unit cell volume changes. Cd^{2+} and Mn^{2+} have larger ionic radii than Cu^+, which may provide larger interstices for the Cu^+ cations to diffuse. The small differences in ionic radii among Zn^{2+}, Co^{2+}, and Cu^+ could also help to rationalize the minimal cation exchange behavior in these systems. Ionic radius comparisons therefore provide a simple proxy for unit cell volumes, as they follow the same trends.

Table 1. Lattice parameters, unit cell volumes, percent differences in unit cell volumes relative to the pseudohexagonal subcell of $Cu_{1.8}S$, and metal cation parameters.

Wurtzite Metal Sulfide	CdS	MnS	$Cu_{1.8}S$	ZnS	CoS
***a, c* (Å)[a]**	4.13, 6.72	3.98, 6.44	3.87, 6.71	3.81, 6.23	3.73, 6.16
Volume (Å³)[b]	99.3	88.4	87.3	78.3	74.2
% Difference in Unit Cell Volume from $Cu_{1.8}S$[c]	–25	–3	0	22	35
Cation radius (pm)[21]	92	80	74	74	72
Metal cation η (eV)[11]	10.29	9.02	6.28	10.88	8.22

[a] The lattice parameters used for $Cu_{1.8}S$ correspond to the pseudohexagonal subcell[5] of the larger triclinic crystal structure.

[b] Unit cell volumes were calculated using the formula for the volume of a hexagonal unit cell: $V = a^2 c \sin(60^\circ)$

[c] Negative values indicate unit cell volume compression relative to the $Cu_{1.8}S$ pseudohexagonal subcell volume, whereas positive values indicate expansion.

The unique behavior in the MnS–CdS system, where both domains exchanged, suggests that additional driving forces could be used to further rationalize the orthogonal exchange chemistry. Solubility of the product phase has been implicated in cation exchange selectivity of heterostructures of copper selenide and copper sulfide.[22] Here, the solubility of MnS (K_{sp} = 5.1 x 10^{-15})[18] is orders of magnitude higher than that of CdS (K_{sp} = 8.0 x 10^{-27}).[5] This suggests that cations being expelled into solution may be more favorable for MnS than CdS, providing additional rationale for why Cu^+ exchange may initially prefer to select for MnS *vs* CdS. This rationale also holds true for ZnS–MnS, as MnS (which selectively exchanges with Cu^+) is much more soluble than ZnS (K_{sp} = 1.6 x 10^{-24}).[5]

Using Janus nanorods that couple together pairwise combinations of four metal sulfides with cations having comparable Pearson's hardness values, we identified selectivities during exchange with Cu^+ cations that were distinct from nanorods of the individual metal sulfides and their physical mixtures. These differences were attributed to the interfaces, with favorable exchanges generating a product containing the metal sulfides that have the best lattice matching, as well as other factors, including unit cell volume compression and solubility. These guidelines can help to predict outcomes of cation exchange reactions on heterostructured nanoparticles that incorporate multiple materials with cations of similar hardness values, as well as to design new types of heterostructured nanoparticles having previously inaccessible features and/or combinations of materials.

This work was supported by the U.S. National Science Foundation under grant DMR-1904122. TEM imaging and STEM-EDS maps were acquired at the Materials Characterization Lab of the Penn State Materials Research Institute.

Conflicts of interest

There are no conflicts to declare.

Notes and references

1 L. De Trizio and L. Manna, *Chem. Rev.*, 2016, **116**, 10852.
2 B.J. Beberwyck, Y. Surendranath, and A.P. Alivisatos, *J. Phys. Chem. C*, 2013, **117**, 19759.
3 M.J. Enright and B.M. Cossairt, *Chem. Commun.*, 2018, **54**, 7109.
4 R.D. Robinson, B. Sadtler, D.O. Demchenko, C.K. Erdonmez, L.-W. Wang, and A.P. Alivisatos, *Science*, 2007, **317**, 355.
5 J.L. Fenton, B.C. Steimle, and R.E. Schaak, *Science*, 2018, **360**, 513.
6 B.C. Steimle, A.M. Fagan, A.G. Butterfield, R.W. Lord, C.R. McCormick, G.A. Di Domizio, and R.E. Schaak, *Chem. Mater.*, 2020, **32**, 5461.
7 R.E. Schaak, B.C. Steimle, and J.L. Fenton, *Acc. Chem. Res.*, 2020, **53**, 2558.
8 J.L. Fenton, B.C. Steimle, and R.E. Schaak, *J. Am. Chem. Soc.*, 2018, **140**, 6771.
9 B.C. Steimle, J.L. Fenton, and R.E. Schaak, *Science*, 2020, **367**, 418.
10 R.G. Pearson, *J. Am. Chem. Soc.*, 1985, **107**, 6801.
11 R.G. Pearson, *Inorg. Chem.*, 1988, **27**, 734.
12 R.G. Parr and R.G. Pearson, *J. Am. Chem. Soc.*, 1983, **105**, 7512.
13 B. Sadtler, D.O. Demchenko, H. Zheng, S.M. Hughes, M.G. Merkle, U. Dahmen, L.-W. Wang, and A.P. Alivisatos, *J. Am. Chem. Soc.*, 2009, **131**, 5285.
14 J.L. Fenton, J.M. Hodges, and R.E. Schaak, *Chem. Mater.*, 2017, **29**, 6168.
15 Z. Li, M. Saruyama, T. Asaka, Y. Tatetsu, and T. Teranishi, *Science*, 2021, **373**, 332.
16 D.-H. Ha, A.H. Caldwell, M.J. Ward, S. Honrao, K. Mathew, R. Hovdan, M.K.A. Koker, D.A. Muller, R.G. Hennig, and R.D. Robinson, *Nano Lett.*, 2014, **14**, 7090.
17 A.G. Butterfield, C.R. McCormick, J.M. Veglak, and R.E. Schaak, *J. Am. Chem. Soc.*, 2021, **143**, 7915.
18 A.E. Powell, J.M. Hodges, R.E. Schaak, *J. Am. Chem. Soc.,* 2016, **138**, 471.
19 J.M. Luther, H. Zheng, B. Sadtler, A.P. Alivisatos, *J. Am. Chem. Soc.,* 2009, **131**, 16851.
20 L. Dloczik, R. Könenkamp, *Nano Lett.,* 2003, **3**, 651.
21 R.D. Shannon, *Acta. Cryst.,* 1976, **A32**, 751.
22 K. Miszta, G. Gariano, R. Brescia, S. Marras, F. e Donato, S. Ghosh, L. De Trizio, L. Manna, *J. Am. Chem. Soc.,* 2015, **137**, 12195.